

# 70-nm-bandwidth achromatic waveguide coupler

Sergio B. Mendes, Lifeng Li, James J. Burke, John E. Lee, and S. Scott Saavedra

We report a general approach to the design of broadband waveguide couplers. A double-parallel grating assembly is used to cancel the first chromatic order, and a proper choice of prism glass and base angle is made to compensate for the second chromatic order. The technique was applied to a Corning glass 7059 waveguide, and a spectral bandwidth of 70 nm was measured by the use of two complementary procedures.

*Key words:* Achromatic coupler, grating coupler, prism coupler, planar waveguide, integrated optics, surface spectroscopy.

## 1. Introduction

Multimode cylindrical waveguides have been widely used for evanescent-wave spectroscopy of interfacial films and optically based chemical sensing.<sup>1-3</sup> An alternative geometry that has seen increasing use is the planar integrated optical waveguide (IOW). Planar IOW's have several advantages over multimode fibers, including a much higher density of total reflection (up to several thousand reflections per centimeter of beam propagation), which yields a concomitant increase in path length. The sensitivity enhancement makes it possible to measure attenuated total reflection (ATR) from interfacial samples that would otherwise be problematic. Examples include dissolved and adsorbed dyes,<sup>4-7</sup> adsorbed protein films,<sup>8,9</sup> and Langmuir-Blodgett films.<sup>10</sup>

The major disadvantage of measuring ATR with planar waveguides is spectral bandwidth. In a given configuration (i.e., launch angle), planar waveguide incouplers are usually efficient for only a narrow spectral range. Thus, to our knowledge, all planar IOW-ATR measurements reported to date have used either a monochromatic source or a narrow spectral band isolated from a polychromatic source.

Different configurations to increase the spectral bandwidth of planar waveguide couplers have been proposed. Spaulding and Morris<sup>11,12</sup> suggested two

different approaches to the problem: (a) a surface-relief transmission grating on top of a prism coupler and (b) a grating coupler combined with a transmission grating tilted at a specific angle. The reported experimental full-widths at half-maximum (FWHM's) were 41 nm and 13 nm for prism-grating and double-grating couplers, respectively. By using a transmission-volume hologram tilted at an angle with respect to a grating coupler, Hetherington *et al.*<sup>13</sup> were able to get a 5-nm bandwidth; Strasser and Gupta<sup>14</sup> achieved a 17-nm bandwidth by combining a grating coupler with a tilted reflecting grating. Recently, Li and Brazas<sup>15</sup> obtained a 45-nm bandwidth by using a prism and a pair of parallel gratings, which greatly simplifies alignment between elements. All experimental demonstrations above rely on canceling the first derivative of the input-coupling angle with respect to wavelength.

In this paper we introduce a different approach to the design of achromatic couplers. Instead of working with coupling angles,<sup>11-14</sup> we describe the achromatization problem as an effective-index-matching process between waveguide and coupler, which is directly related to coupling efficiency.<sup>16</sup> The effective-index mismatch function is defined and expanded into a Taylor series in which the coefficients are defined as chromatic orders. The achromatization process takes place through correction of increasingly higher orders. The method is general and can be applied to any specific configuration with the appropriate description of the effective index for each coupler.

We follow the general configuration of Li and Brazas,<sup>15</sup> but we search for a design that corrects not only the first but also the second chromatic order by making use of available parameters that have not been previously exploited in the configuration. The structure shown in Fig. 1, which combines two grat-

---

S. B. Mendes, L. Li, and J. J. Burke are with the Optical Sciences Center, University of Arizona, Tucson, Arizona 85721. J. E. Lee and S. S. Saavedra are with the Department of Chemistry, University of Arizona, Tucson, Arizona 85721. E-mail may be addressed to sermende@ccit.arizona.edu.

Received 30 November 1994; revised manuscript received 6 March 1995.

0003-6935/95/276180-07\$06.00/0.

© 1995 Optical Society of America.

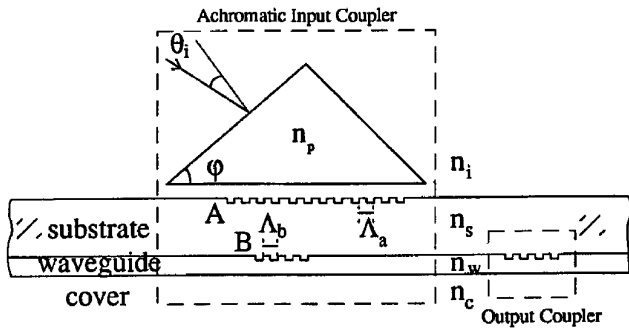


Fig. 1. Schematic representation of overall structure and symbols used for each element.

ings and a prism, has simplicity and sufficient degrees of freedom. The two gratings are parallel to the waveguide, avoiding the critical alignment required in previous designs,<sup>11–14</sup> and can be fabricated on a single slide. As we show below, the gratings are designed with slightly different spatial frequencies to function as an equivalent long-period grating, and their linear wavelength dependence is used to correct the first chromatic order. The prism offers the degrees of freedom (choices of glass and base angle) needed to correct the second chromatic order. From an improved design we were able to extend the input-coupling spectral bandwidth much beyond that of previously reported experiments.<sup>12–15</sup>

## 2. Theory

The problem of broadband coupling into a planar waveguide can be simply formulated in terms of the matching of the effective index (or  $\beta$ , the projection of wave vector along the direction of mode propagation) of the waveguide with that of the coupler (prism, grating, or combination) for a broad spectral range. For this purpose we define an effective-index mismatch function  $F$  as the difference between waveguide and coupler effective indices:

$$F(\lambda) \equiv N_w(\lambda) - N_p(\lambda) - N_g(\lambda), \quad (1)$$

where each term on the right-hand side is defined, referring to Fig. 1, as follows:

(a)  $N_w$  is the waveguide effective index obtained from the well-known characteristic equation

$$\begin{aligned} \frac{2\pi}{\lambda} t_w (n_w^2 - N_w^2)^{1/2} \\ = m\pi + \tan^{-1} \left[ \frac{\left( \frac{n_w}{n_c} \right)^{2\rho} \left( N_w^2 - n_c^2 \right)^{1/2}}{\left( n_w^2 - N_w^2 \right)} \right] \\ + \tan^{-1} \left[ \frac{\left( \frac{n_w}{n_s} \right)^{2\rho} \left( N_w^2 - n_s^2 \right)^{1/2}}{\left( n_w^2 - N_w^2 \right)} \right], \quad (2) \end{aligned}$$

where  $\rho = 0$  applies to TE<sub>m</sub> modes and  $\rho = 1$  applies to TM<sub>m</sub> modes. We note that Eq. (2) has an explicit wavelength dependence and an implicit dependence due to the dispersion of materials involved.

(b) The effective index  $N_g$  for the two gratings, A and B, which are aligned parallel with the waveguide, is described by

$$N_g = m_a \frac{\lambda}{\Lambda_a} + m_b \frac{\lambda}{\Lambda_b} \equiv \frac{\lambda}{\Lambda^*}, \quad (3)$$

where  $\Lambda^*$  is an equivalent grating period. We restrict ourselves below to the first diffraction orders by assuming that  $m_a = -1$  and  $m_b = +1$ . Note that the grating term gives only a linear wavelength contribution.

(c) From simple geometry and Snell's law, the effective index  $N_p$  of the prism is given by

$$N_p = n_i \sin \theta_i \cos \varphi + (n_p^2 - n_i^2 \sin^2 \theta_i)^{1/2} \sin \varphi. \quad (4)$$

To search for a solution over a broad spectral range, the mismatch function  $F$  is expanded in a Taylor series centered at the wavelength of interest ( $\lambda_0$ ):

$$F(\lambda) \cong F(\lambda_0) + \frac{dF}{d\lambda} \Big|_{\lambda_0} (\lambda - \lambda_0) + \frac{d^2F}{d\lambda^2} \Big|_{\lambda_0} \frac{(\lambda - \lambda_0)^2}{2} + O(\Delta\lambda^3). \quad (5)$$

Setting the zero-, first-, and second-order coefficients to zero yields

$$\begin{aligned} F(\lambda_0) = N_w - n_i \sin \theta_i \cos \varphi - (n_p^2 - n_i^2 \sin^2 \theta_i)^{1/2} \\ \times \sin \varphi - \frac{\lambda_0}{\Lambda^*} = 0, \quad (6) \end{aligned}$$

$$\frac{dF}{d\lambda} \Big|_{\lambda_0} = \frac{dN_w}{d\lambda} - \frac{n_p \sin \varphi}{(n_p^2 - n_i^2 \sin^2 \theta_i)^{1/2}} \frac{dn_p}{d\lambda} - \frac{1}{\Lambda^*} = 0, \quad (7)$$

$$\begin{aligned} \frac{d^2F}{d\lambda^2} \Big|_{\lambda_0} = \frac{d^2N_w}{d\lambda^2} - \frac{n_p \sin \varphi}{(n_p^2 - n_i^2 \sin^2 \theta_i)^{1/2}} \frac{d^2n_p}{d\lambda^2} \\ + \frac{n_i^2 \sin^2 \theta_i \sin \varphi}{(n_p^2 - n_i^2 \sin^2 \theta_i)^{3/2}} \left( \frac{dn_p}{d\lambda} \right)^2 = 0. \quad (8) \end{aligned}$$

Equation (6) is the usual coupling condition for a particular wavelength. Making the first chromatic order zero [Eq. (7)] gives a stable solution around the design wavelength, and setting the second-chromatic-order coefficient [Eq. (8)] to zero enlarges the coupling region.

Thus the problem of designing an achromatic coupler for a specific waveguide consists of searching for values of the angle of incidence  $\theta_i$ , equivalent grating period  $\Lambda^*$ , index of refraction  $n_p$  of the prism, and base angle  $\varphi$  that simultaneously cancel the first three coefficients in the Taylor series. We used a simple approach for solving the system of coupled equations by initially selecting a specific glass and neglecting the grating term ( $N_g = 0$  or  $\Lambda^* = \infty$ ). The incident coupling angle  $\theta_i$  and the prism base angle  $\varphi$  were then calculated by simultaneously solving Eqs.

(6) and (8). The grating parameter  $\Lambda^*$  was then obtained from the first-order Eq. (7). Of course when a grating term ( $N_g \neq 0$ ) is introduced we must recalculate. However, as the grating contribution is generally small, usually one or two additional iterations are sufficient for the variables to converge to the achievable experimental precision. Several glass materials were tested, and only certain choices with the appropriate index of refraction and Abbe number yielded a solution for our particular waveguide.

On correction up to the second chromatic order, the effective-index mismatch function exhibits a cubic wavelength dependence. We then define a merit function to be the sum of squares of the mismatch function over the spectral region of interest and minimize the function by refining the variables. Basically the final procedure compensates the cubic contribution by reintroducing a small amount of the first-order term with the opposite sign. This is analogous to the usual procedure in lens design that is used to initially correct third-order aberrations (Seidel aberrations); when fifth-order terms subsequently become dominant, small amounts of the third order with the opposite sign are reintroduced for balancing.

The procedure was implemented into a computer code for an automatic search of solutions. The dispersion of all the materials involved has been taken into account as well as the explicit wavelength dependence of the grating and waveguide effective indices. As usual in the waveguide case,  $N_w$  and its derivatives are calculated by the use of a numerical routine.

In Fig. 2 examples of the effective-index mismatch function for four different couplers are given: a single-grating coupler, a prism coupler, the achromatic design specified in Li and Brazas,<sup>15</sup> and our achromatic design, which is corrected up to the

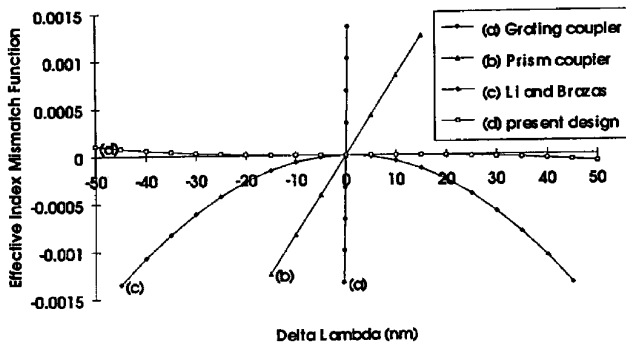


Fig. 2. Comparison of effective-index mismatch function for different incoupler designs: (a) grating coupler  $\Lambda = 313.4$  nm; (b) prism coupler with  $\text{LaSF}_3$  glass and base angle  $52.206^\circ$ ; (c) Li and Brazas<sup>15</sup> double grating  $\Lambda_a = 309.5$  nm and  $\Lambda_b = 308.8$  nm, prism  $\text{SF}_1$  glass, base angle  $60^\circ$ ; (d) present design, with double grating  $\Lambda_a = 305.4$  nm and  $\Lambda_b = 313.4$  nm, prism  $\text{LaSF}_3$  glass, base angle  $52.206^\circ$ . For all designs, the waveguide material is Corning glass 7059 with a thickness of 400 nm, the cover is air, and TE polarization is assumed. Designs (a), (b), and (d) are centered at  $\lambda_0 = 550$  nm, and the substrate is fused silica; for design (c)  $\lambda_0 = 685$  nm, and the substrate is pyrex.

second chromatic order. For the grating and prism couplers where no achromatization has been attempted, a strong linear dependence rapidly increases the mismatch function for small detunings of the design wavelength. In the design of Li and Brazas, where the first order has been canceled, a quadratic behavior is observed. The mismatch function of our design shows a weak cubic dependence and is kept to small values over a much broader region.

Waveguide thickness is another parameter that can be included in the design process. It should be noted that we were able to correct the first chromatic order of a conventional prism coupler merely by adjusting waveguide thickness. Though its mismatch function is inferior to the achromatic design, it nonetheless represents an important improvement over the conventional prism or grating couplers and can be used for certain applications.

Our condition for canceling the first derivative of the mismatch function with respect to wavelength is equivalent to the condition given by Spaulding and Morris,<sup>11</sup> which imposes a zero derivative of the incident coupling angle with respect to wavelength ( $d\theta_i/d\lambda = 0$ ). This can be verified by taking our mismatch function as an implicit function of wavelength and coupling angle and setting it equal to zero,

$$F(\lambda, \theta_i) = 0, \quad (9)$$

so we can write the following relation:

$$\frac{d\theta_i}{d\lambda} = -\frac{\partial F/\partial \lambda}{\partial F/\partial \theta_i}. \quad (10)$$

We conclude that, if the angular variation against wavelength is zero, the first derivative of the effective-index mismatch function with respect to wavelength is also zero.

From the effective-index mismatch function  $F$  we calculate the normalized coupling efficiency, following Brazas and Li.<sup>16</sup> The functional form is simple when one of the length parameters involved (grating length  $L_g$ , beam size  $\omega_0$ , or  $L_c \equiv 1/\alpha$ , where  $\alpha$  is the waveguide leakage rate) is much smaller than the others. In Table 1 the expressions for each limiting case are given, where we have used  $\Delta\beta(\lambda) \equiv (2\pi/\lambda)F(\lambda)$ . Unlike previous studies<sup>11-14</sup> that used the incident coupling angle, here there exists a straightforward connection between the design function  $F(\lambda)$  and the variable  $\eta(\lambda)$  that is experimentally determined.

### 3. Fabrication and Experiment

A prism satisfying our conditions was manufactured from  $\text{LaSF}_3$  Schott glass ( $n_d = 1.80801$  and  $\nu_d = 40.61$ ) with a base angle of  $52.206^\circ$ .

Table 1. Normalized Coupling Efficiency for Each Limiting Case

Condition	Normalized Coupling Efficiency ( $\eta$ )
$L_g \ll L_c, L_g \ll \omega_0$	$\text{sinc}^2(\Delta\beta L_g/2)$
$L_c \ll L_g, L_c \ll \omega_0$	$\alpha^2/(\alpha^2 + \Delta\beta^2)$
$\omega_0 \ll L_g, \omega_0 \ll L_c$	$\exp[-(1/2)(\Delta\beta\omega_0)^2]$

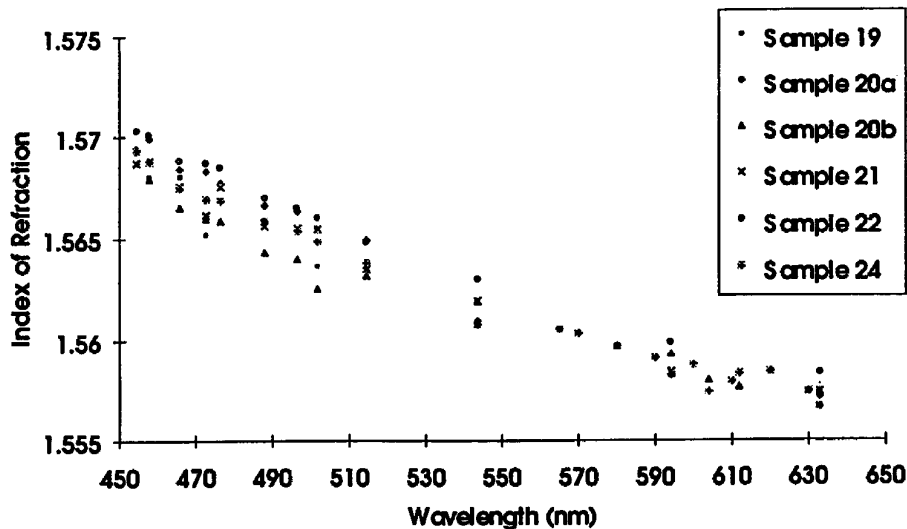


Fig. 3. Measured index of refraction versus wavelength for several Corning glass 7059 films fabricated by the use of sputtering deposition.

The grating fabrication follows the procedure reported in Li *et al.*<sup>17</sup> We used the 441.65-nm line of a Kimmon He–Cd laser that was expanded, spatially filtered, and collimated. The intensity for the expanded beam was 0.38 mW/cm<sup>2</sup>, and the photoresist was exposed for 45 s. A real-time control of diffraction efficiency gave an optimum time of 90 s for the development process. The photoresist grating pattern was transferred to the fused-silica substrate by the use of a reactive-ion-milling process that uses freon gas.

On the fused-silica slide that was to be coated with the waveguide, two gratings separated by 12.5 mm were fabricated; one grating was part of the input achromatic coupler (see Fig. 1), and the other was used as a simple output coupler for power measurements. We determined the grating period of the input coupler to be  $\Lambda_b = 313.4$  nm by measuring the diffraction angle in Littrow configuration.

The waveguide was Corning glass 7059 deposited on fused-silica substrates (50.8 cm × 2.54 cm) with a Perkin-Elmer 2400 RF diode-sputtering system. The bias voltage on the material target was set to 1150 V, and a power of 250 W was established for a pressure of  $3.9 \times 10^{-3}$  Torr in the chamber. The predeposition vacuum was  $2 \times 10^{-6}$  Torr, and a reactive atmosphere of Ar (70%) and O<sub>2</sub> (30%) was dynamically controlled during deposition by the use of an MKS two-channel flowmeter. We measured a  $400 \pm 2$  nm thickness for the waveguide used in our experiment and estimated an average deposition rate of 49.5 Å/min. Many samples have been prepared under the same condition for a precise characterization of the material dispersion as required for design purposes. In Fig. 3 we present the dispersion results for several 7059 waveguides obtained from prism-coupler measurements, from which a standard deviation of less than  $\pm 0.001$  in the characterization of the index of refraction was determined. Typical loss was 2 dB/cm at  $\lambda = 633$  nm.

On a second fused-silica slide another grating with a spatial period  $\Lambda_a = 306.2$  nm, which closely approximates the design value ( $\Lambda_a = 305.4$  nm, as indicated in Fig. 2), was fabricated.

The two slides were brought into contact from the unworked sides by an index-matching liquid of refractive index 1.46. After the grooves were optically aligned the two slides were glued together, creating a laminate structure, as shown in Fig. 1, with overall thickness of 2.0 mm. The equivalent grating period  $\Lambda^*$  obtained from the combined pair was 13,328 nm. A liquid with a high index of refraction (1.80) was used to bring the prism and grating A into contact.

Figure 4 illustrates the experimental setup used in the coupling-efficiency measurements. To cover a broad spectral range, a Coherent Innova 70 argon-ion laser, a Coherent CR-599 dye (Couramin C6) laser scanning from 525 to 580 nm, and a Melles-Griot He–Ne laser were used as sources. Special attention was paid to guarantee that beams from different sources reached the input coupler at the same posi-

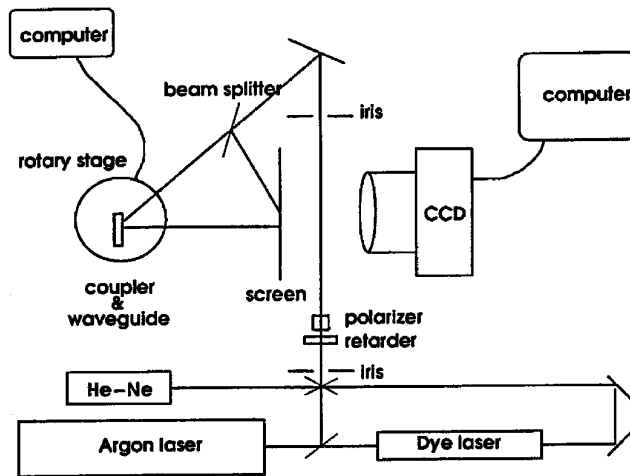


Fig. 4. Experimental setup for coupling-efficiency measurements.

tion and direction by sending them through two irises separated by 1.05 m. Transverse electric (TE) polarization was selected with a Glan–Thompson polarizer. The waveguide and the coupler were mounted on a rotary stage driven by a stepper motor, and angular measurements were digitally controlled. After being coupled in and propagated through the waveguide, the guided mode was coupled out by a single-grating outcoupler and projected on a screen. A reference signal was collected from the beam with a spectrally neutral beam splitter and directed to the same screen. Both spots were simultaneously photographed with a CCD camera (Photometrics CH210 with Tektronix TK512CB/AR chip).

#### 4. Results and Discussion

We initially measured the dependence of coupling efficiency on angle of incidence for several discrete wavelengths. Two different incouplers were investigated: the achromatic coupler designed and fabricated as described above and a conventional grating coupler with spatial frequency  $\Lambda = 313.4$  nm. Figure 5A shows the results for the achromatic coupler; the angular dependence of coupling efficiency was measured at 525, 550, and 580 nm. Strong overlap between all three curves is observed, with the 525- and the 580-nm curves intersecting at 87% of the normalized coupling efficiency. An otherwise equivalent measurement was made for the single-grating

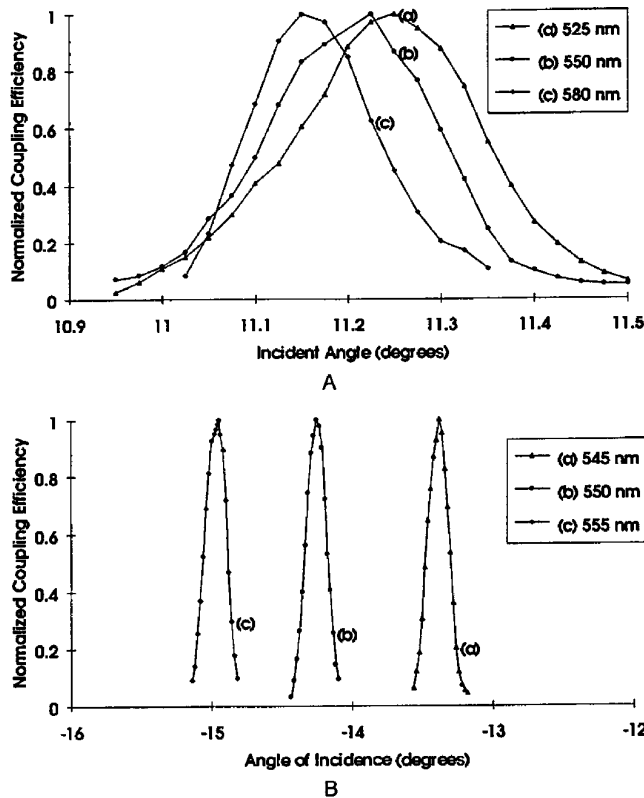


Fig. 5. Dependence of coupling efficiency on angle of incidence for A, our achromatic waveguide coupler at three particular wavelengths,  $\lambda = 525, 550,$  and  $580$  nm, and B, a conventional grating coupler at three particular wavelengths,  $\lambda = 545, 550,$  and  $555$  nm.

coupler at 545, 550, and 555 nm. In contrast, Fig. 5B illustrates that a spectral separation of only 5 nm can split apart the coupling-efficiency curves, and the overlap is negligible.

From the measured angular separation of these lines ( $d\theta_i/d\lambda$ ) and the angular bandwidth ( $\Delta\theta_{50\%}$ ), the spectral bandwidth is estimated with

$$\Delta\lambda_{50\%} = \Delta\theta_{50\%} \left| \frac{\partial F / \partial \theta_i}{\partial F / \partial \lambda} \right| = \frac{\Delta\theta_{50\%}}{|d\theta_i/d\lambda|}, \quad (11)$$

yielding  $\Delta\lambda_{50\%} = 97$  nm for the achromatic coupler and  $\Delta\lambda_{50\%} = 1.1$  nm for the conventional grating coupler.

A direct measurement of coupling efficiency over the spectral range of interest was also performed. The procedure here was to initially adjust beam location and to tune the angle of incidence for a maximum of the coupled power into the waveguide at the center wavelength (550 nm). We then performed all measurements by tuning the wavelength without any further change in the configuration. The measured input-coupling angle  $\theta_i$  was  $11.25^\circ \pm 0.12^\circ$ , in excellent agreement with the expected theoretical value ( $11.26^\circ$ ). The estimated absolute input-coupling efficiency was 0.04%, because of the low diffraction efficiency of grating A that was used in the present demonstration and the mismatch between the grating-coupler leakage rate ( $\alpha$ ) and the spot size of the input beam.

Figure 6 shows the measured normalized coupling efficiency for the achromatic coupler as a function of wavelength. A spectral bandwidth (FWHM) of 70 nm was obtained. Also plotted is the coupling efficiency predicted from the effective-index mismatch function  $F$  when the inverse of the waveguide leakage rate ( $L_c \equiv 1/\alpha$ ) is estimated to be the shortest of the length parameters (see Table 1). Although the results are satisfactory for the region close to the central wavelength, they clearly disagree at the sidebands. However, as pointed out by Strasser and Gupta,<sup>14</sup> lateral shift of the beam as a function of wavelength (illustrated in Fig. 7) plays an important role for large deviations from the central wavelength.

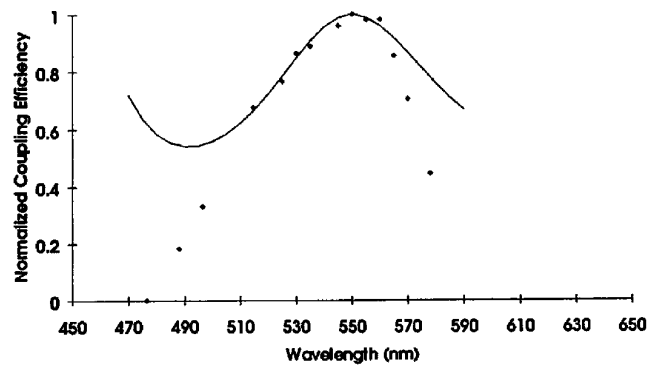


Fig. 6. Normalized coupling efficiency for an achromatic coupler as a function of wavelength. Experimental results ( $\blacklozenge$ ) and theoretical calculation (solid curve) are shown without consideration of lateral shift effects.

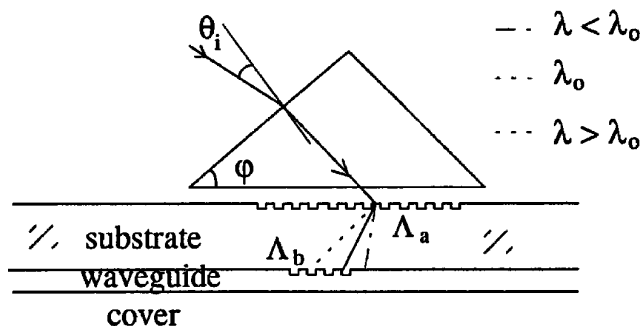


Fig. 7. Schematic representation of lateral shift for different wavelengths.

The expressions in Table 1, which are used for the theoretical calculation of coupling efficiency, take into account only the effect of phase mismatch and do not consider lateral displacement of the beam with respect to the central wavelength. We calculate for our achromatic coupler a lateral shift of  $\pm 0.12$  mm for detuning of  $\pm 25$  nm from the central wavelength, mainly because of grating A and a negligible contribution from the prism. Shorter wavelengths are shifted toward a region without grating modulation, and longer wavelengths are moved inside the grating and far from the edge. In the former case the coupling efficiency is reduced because only part of the beam is diffracted into the waveguide; in the latter case a longer propagation length inside the grating increases losses as a result of outcoupling. Both cases tend to reduce coupling efficiency and become the dominant effect, rather than phase mismatch, at substantial deviations from the central wavelength. However, this lateral shift can be substantially reduced by the use of a much thinner substrate and longer spatial frequencies for the gratings (with the same equivalent grating period  $\Lambda^*$ ).

## 5. Conclusion

We have described a simple and straightforward approach to the design of achromatic waveguide couplers based on correction of chromatic orders obtained from a Taylor series expansion of the effective-index mismatch function. The formulation is applied to a prism-double-grating achromatic coupler, and for the first time to our knowledge a design that corrects up to the second chromatic order was experimentally implemented. A spectral bandwidth of 70 nm was measured, which is substantially greater than previous reported values.<sup>12-15</sup>

Based on programmatic considerations, we have focused our attention on increasing the bandwidth of the waveguide coupler, leaving the absolute coupling efficiency aside. Such an approach is justified because the absolute efficiency of the proposed coupling device can be improved without affecting its bandwidth. Additionally, for many applications in chemical sensors, the efficiency that we report here is adequate. If necessary, a higher absolute efficiency can be obtained by choosing appropriate groove depths

of gratings A and B for maximum diffraction efficiency and optimum matching between beam size and leakage rate, respectively.

As currently practiced, planar waveguide ATR is a highly sensitive spectrometric technique for characterization of thin films and interfaces. The achromatic coupler presented here shows considerable potential for extending planar waveguide IOW-ATR to the broadband regime. Development of a technology to acquire broadband ATR spectra at the surface of a planar IOW would find immediate application in at least two important areas: (a) spectral characterization of interfacial organic and biological thin-film assemblies, particularly at solid-liquid interfaces, and (b) simultaneous chemical sensing of multiple analytes at spectrally resolved wavelengths, based on increased information content available in the polychromatic domain.

This work has been supported by the National Science Foundation under grant CHE-9403896 and the National Institutes of Health under grant R03 RR08097. Sergio B. Mendes gratefully acknowledges support from Coordenação de Aperfeiçoamento de Pessoal de Nível Superior (Brazilian Agency Supporting Graduate Programs).

## References

- O. S. Wolfbeis, "Fiber-optic sensors in biomedical sciences," *Pure Appl. Chem.* **59**, 663-672 (1987).
- R. E. Dessey, "Waveguides as chemical sensors," *Anal. Chem.* **61**, 1079A-1094A (1989).
- M. A. Arnold, "Fiber-optic chemical sensors," *Anal. Chem.* **64**, 1015A-1025A (1992).
- J. N. Polky and J. H. Harris, "Absorption from thin-film waveguides," *J. Opt. Soc. Am.* **62**, 1081-1087 (1972).
- S. S. Saavedra and W. M. Reichert, "Integrated optical attenuated total reflection spectrometry of aqueous superstrates using prism-coupled polymer waveguides," *Anal. Chem.* **62**, 2251-2256 (1990).
- M. D. DeGrandpre, L. W. Burgess, P. L. White, and D. S. Goldman, "Thin film planar waveguide sensor for liquid phase absorbance measurements," *Anal. Chem.* **62**, 2012-2017 (1990).
- D. A. Stephens and P. W. Bohn, "Absorption spectrometry of bound monolayers on integrated optical structures," *Anal. Chem.* **61**, 386-390 (1989).
- S. S. Saavedra and W. M. Reichert, "In situ quantitation of protein adsorption density by integrated optical waveguide attenuated total reflection spectrometry," *Langmuir* **7**, 995-999 (1991).
- D. S. Walker, M. D. Garrison, and W. M. Reichert, "Protein adsorption to HEMA/EMA copolymers studied by integrated optical techniques," *J. Colloid Interface Sci.* **157**, 41-49 (1993).
- T. E. Plowman, M. D. Garrison, D. S. Walker, and W. M. Reichert, "Surface sensitivity of SiON integrated optical waveguides (IOWs) examined by IOW-attenuated total reflection spectrometry and IOW-Raman spectroscopy," *Thin Solid Films* **243**, 610-615 (1994).
- K. E. Spaulding and M. Morris, "Achromatic waveguide input/output coupler design," *Appl. Opt.* **30**, 1096-1112 (1991).
- K. E. Spaulding and M. Morris, "Achromatic waveguide couplers," *J. Lightwave Technol.* **10**, 1513-1518 (1992).

13. D. L. Hetherington, R. K. Kostuk, and M. C. Gupta, "Dispersion compensation for an integrated optic grating coupler utilizing a transmission volume hologram," *Appl. Opt.* **32**, 303–308 (1993).
14. T. A. Strasser and M. C. Gupta, "Grating coupler dispersion compensation with a surface-relief reflection grating," *Appl. Opt.* **33**, 3220–3226 (1994).
15. L. Li and J. C. Brazas, "A method for achromatically coupling a beam of light into a waveguide," U.S. patent 5,420,947 (30 May 1995).
16. J. C. Brazas and L. Li, "Analysis of input-grating couplers having finite lengths," *Appl. Opt.* **34**, 3786–3792 (1995).
17. L. Li, M. Xu, G. I. Stegeman, and C. T. Seaton, "Fabrication of photoresist masks for submicrometer surface relief gratings," in *Integrated Optical Circuit Engineering V*, M. A. Mentzer, ed., *Proc. Soc. Photo-Opt. Instrum. Eng.* **835**, 72–82 (1987).